Biochemical and Biophysical Research Communications 387 (2009) 585–589

Contents lists available at ScienceDirect

Biochemical and Biophysical Research Communications

journal homepage: www.elsevier.com/locate/ybbrc

Real-time neuronal homeostasis by coordinating VGSC intrinsic properties

Rongjing Ge [a,b], Na Chen [a], Jin-Hui Wang [a,b,*]

[a] Department of Physiology, Bengbu Medical College, Anhui 233000, China
[b] State Key Labs for Brain and Cognitive Sciences, Institute of Biophysics, Chinese Academy of Sciences, Beijing 100101, China

ARTICLE INFO

Article history:
Received 7 July 2009
Available online 17 July 2009

Keywords:
Homeostasis
Neuron
Action potential
Threshold potential
Refractory period and sodium channel

ABSTRACT

Homeostasis of internal environment and cellular metabolism ensures cells' functions to be stable in living organisms. Cellular homeostasis is believed to be maintained via feedback or feedforward manners. We report a novel mechanism that maintains neuronal homeostasis through coordinating the intrinsic properties of single molecules concurrently. Spike encoding and sodium channel dynamics at cortical neurons were studied by patch-clamp recording. Voltage-gated sodium channels set refractory period and threshold potential toward different directions to stabilize the energetic barrier for firing sequential action potentials. This neuronal homeostasis is not affected by intracellular Ca^{2+} signals and membrane potentials. Real-time homeostasis maintains precise and reliable neuronal encoding without any destabilization.

Introduction

Neurons encode meaningful signals precisely for well-organized behaviors and cognition, in which their functional state has to be stabilized. Neuronal activities undergo homeostatic change during pharmacological or genetic manipulations [1,2], e.g., neuronal excitability shifts to opposite direction after removing specific treatments [3–5]. This homeostasis to stabilize neuronal functions emerges slowly via regulating gene expression. In addition to this feedback pattern, homeostasis can be rapidly recruited by coordinating the functions of subcellular compartments in a feedforward manner, in which intracellular Ca^{2+} is a primary coordinator [6]. These types of neuronal homeostasis maintain reliable and precise encoding; however, they are subjected, more or less, to be a delayed onset.

Homeostasis at the neurons is ideally established in real-time manner to prevent their encoding from any instability and to allow their encoded signals coordinating well-organized behaviors in time. In terms of its mechanism, resetting molecule's properties toward different directions synchronously to balance a specific function should maintain real-time neuronal homeostasis. To this hypothesis, we have examined whether voltage-gated sodium channels (VGSCs) reset threshold potentials and refractory periods, which are "energetic barriers" of firing action potentials [7,8], toward opposite directions to enable the neurons encode spikes consistently. VGSC dynamics and neuronal intrinsic properties were measured by patch-clamp recordings in cortical slices.

Methods and materials

Cortical slices (400 μm) were prepared from FVB-Tg(Gad-GFP)45704Swn/J mice whose GABAergic neurons express enhanced green fluorescent protein (eGFP). Mice in postnatal day 15–20 were anesthetized by injecting chloral hydrate (300 mg/kg) and decapitated with a guillotine. The slices were cut with a Vibratome in the modified and oxygenized (95% O_2/5% CO_2) artificial cerebrospinal fluid (mM: 124 NaCl, 3 KCl, 1.2 NaH_2PO_4, 26 $NaHCO_3$, 0.5 $CaCl_2$, 5 $MgSO_4$, 10 dextrose and 5 Hepes; pH 7.35) at 4 °C, and then were held in the normal oxygenated ACSF (mM: 124 NaCl, 3 KCl, 1.2 NaH_2PO_4, 26 $NaHCO_3$, 2.4 $CaCl_2$, 1.3 $MgSO_4$, 10 dextrose and 5 Hepes; pH 7.35) 25 °C for 1–2 h before experiments. A slice was transferred to the submersion chamber (Warner RC-26G) that was perfused with the normal ACSF at 31 °C for the electrophysiological experiments [9]. The entire procedures were approved by Institutional Animal Care Unit Committee in Beijing China.

GFP-labeled GABAergic neurons in layer II–IV of the cerebral cortex were selected for our studies. These neurons are a round/ovary-like soma and tree branch-like dendrites under DIC optics (Nikon FN-600). As these neurons are labeled with eGFP, their morphology can be seen under fluorescent microscopy with an excitation wavelength at 488 nm and emission wavelength at 525 nm. These interneurons were recorded by patch-clamp in either whole-cell membrane potentials or single channel currents.

Abbreviations: Vts, threshold potential; ARP, absolute refractory period; VGSC, voltage-gated sodium channels.

* Corresponding author. Address: State Key Labs for Brain and Cognitive Sciences, Institute of Biophysics, Chinese Academy of Sciences, Beijing 100101, China.
E-mail address: jhw@sun5.ibp.ac.cn (J.-H. Wang).

0006-291X/$ - see front matter © 2009 Elsevier Inc. All rights reserved.
doi:10.1016/j.bbrc.2009.07.066

Action potentials were recorded by multi-clamp 700B and their signals were inputted into pClamp-9 (Axon Instrument INC, Foster, CA, USA). In our experiments, transient capacitance was compensated, and output bandwidth was 3 kHz. The standard pipette solution contained (mM) 150 K-gluconate, 5 NaCl, 0.4 EGTA, 4 Mg-ATP, 4 Na-phosphocreatine, 0.5 Tris-GTP and 10 Hepes (pH 7.4 adjusted by 2 M KOH). Fresh pipette solution was filtered with 0.1 μm centrifuge filter before the use. The osmolarity of the pipette solution was 295–305 mOsmol, and the pipette resistance was 6–8 MΩ.

Neuronal intrinsic properties measured in our study include refractory periods after each spike and threshold potentials for its subsequent spike. Absolute refractory period of spike one (ARP1) is measured by injecting two depolarization pulses (3 ms in duration and 5% above threshold in intensity) into the neurons, in which pulse one induces spike one at 100% firing probability and inter-pulse intervals are adjusted to have pulse two inducing spike two at 50% probability. The duration between spikes one and two is defined as ARP1 (Fig. 1A and [7]). Moreover, the ARPs of sequential action potentials are measured by injecting multiple depolarization pulses (3 ms and 5% above threshold) into the neurons (Fig. 1B). In the measurement of ARPs for these spikes, they appear complete in amplitude and are just out of relative refractory periods of their preceding spikes (Fig. 1B). By adjusting inter-pulse intervals similar to ARP1 measurement, we read out the durations from complete spikes to their subsequent spikes with 50% probability, i.e., the ARP of sequential spikes (Fig. 1B and [6,7]). Threshold potentials for spike initiation at ARP are the voltages of firing spikes at 50% probability [7], such as Vts1 (Fig. 1A) and Vts3 (Fig. 1B).

The currents from single VGSCs were recorded in cell-attached configuration with the multi-clamp 700B and pClamp-9 at the neurons of cortical slices. Seal resistance was above 10 GΩ, and pipette resistance was 10–15 MΩ. Pipette solution contains (mM) 120 NaCl, 2 $MgCl_2$, 10 Hepes, 30 TEA and 0.1 mibefradil. TEA and mibefradil were used to block voltage-gated potassium and type-T calcium channels, respectively. Threshold potentials for VGSC activation were measured by adding negative voltage pulses (5 ms) to the recording pipettes, and refractory periods for VGSC reactivation were measured by altering inter-pulse intervals in 4–13 ms.

Data were analyzed if the recorded neurons showed the resting membrane potentials negatively more than −60 mV. In addition, the criteria for the acceptation of experimental data included less than 5% changes in resting membrane potential, spike magnitude, input/seal resistance during each experiment. Input resistance was monitored by measuring cellular responses to hyperpolarization pulses at the same values as the depolarization that evoked spikes. Data for single channel recording was taken into account when seal resistance was larger than 10 GΩ. The values of spike amplitudes, ARP, uEPSCs and VGSC currents are presented as mean ± SE. The comparisons between groups are done by *t*-test.

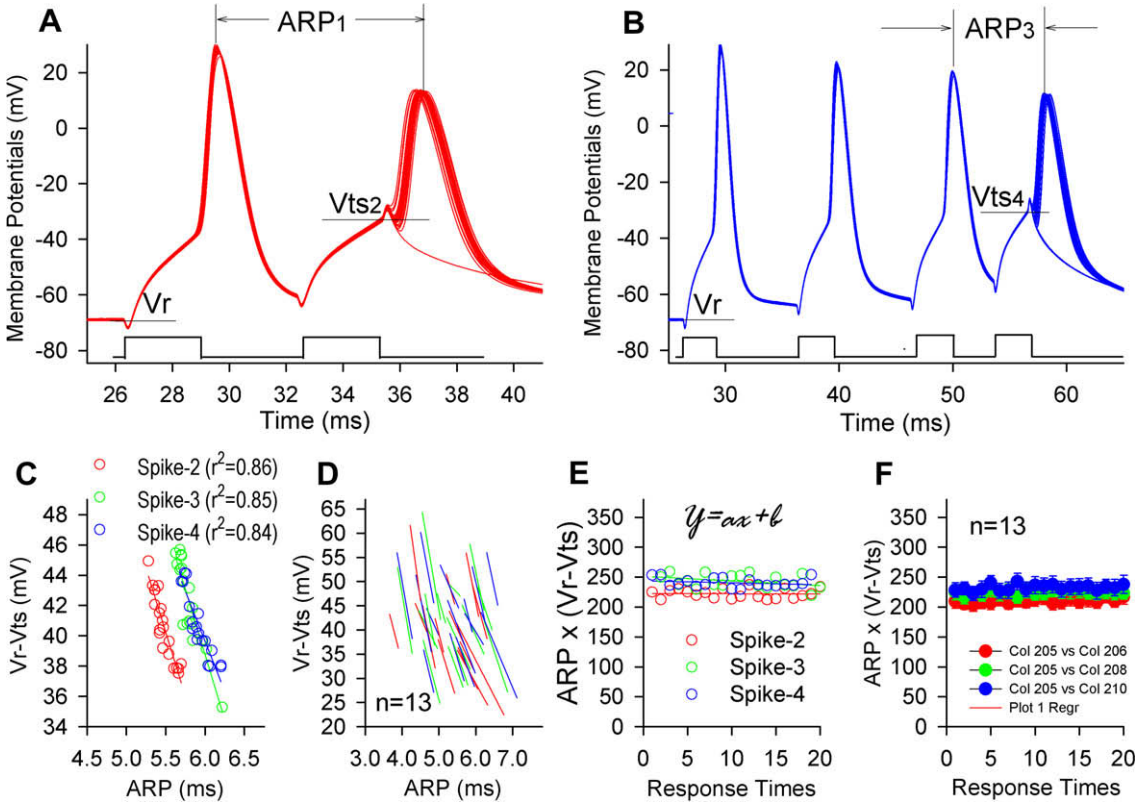

Fig. 1. Inverse correlation between ARP and Vts sets constant energetic barrier for firing action potentials at GABAergic neurons. Depolarization current pulses (5% above threshold stimuli in intensity and 3 ms in duration) used to measure ARPs and Vts are presented at the bottom of waveforms of action potentials. (A) A plot illustrates superimposed waveforms in the measurements of ARP for spike-1 and Vts for spike-2 at a neuron. These two parameters determine spike-2 initiation. (B) A plot shows superimposed waveforms in the measurements of ARP for spike-3 and Vts for spike-4 at this neuron. These two parameters determine an initiation of spike-4. (C) Inverse correlations between ARP1 and Vts2 (red symbols and line), ARP2 and Vts3 (green), as well as ARP3 and Vts4 (blue) from the neuron in (A) and (B. (D) Inverse correlations between ARP1 and Vts2 (red lines), ARP2 and Vts3 (green), as well as ARP3 and Vts4 (blue) from other neurons (n = 13). (E) The energetic barrier (ARP * Vts) versus response time of spike-2 (red symbols and line), spike-3 (green) and spike-4 (blue) from the neuron in (A)–(C). (F) Energetic barrier versus response time of spike-2 (red symbols), spike-3 (green) and spike-4 (blue) averaged from all of the neurons (n = 14). In the measurements of ARP and Vts, the spikes at the end of ARP were induced with seventy times of current pulses in each single neuron. (For interpretation of the references to color in this figure legend, the reader is referred to the web version of this paper.)

Results

Each firing in sequential action potentials is controlled by the absolute refractory period (ARP) of the preceding spike and the threshold potential (Vts), in which Vts denotes neuronal sensitivity to inputs, and ARP is a time delay for the neurons to be reactivated. These two factors mediated by VGSCs make up the energetic barrier for firing sequential spikes [7], which we define as a multiplication of ARP and Vts. Constant values in this energetic barrier overtime confer the homeostatic encoding of neuronal signals.

We analyzed the relationship between ARP and Vts, and calculated the energetic barrier to fire sequential action potentials. Fig. 1A and B shows the measurements of ARPs for spikes one and three, as well as of Vts for their subsequent spikes at ARP (see Materials and methods and [7] for detail) by giving hundred times of depolarization pulses into a single neuron. Values for ARP and Vts appear fluctuated overtime, but the longer ARPs are associated with the lower Vts, or vice versa, in corresponding pairs. There are inverse and linear correlations between ARP1 and Vts2 (red symbols and line), between ARP2 and Vts3 (green), as well as between ARP3 and Vts4 (blue) in this neuron (Fig. 1C, $r^2 > 0.8$, $p < 0.01$). Such correlations are also observed in other neurons ($n = 13$ in Fig. 1D). The result indicates that the fluctuations in neuronal sensitivity and readiness for reactivation at given time are intrinsically associated in an inverse manner.

Interestingly, the energetic barriers for each of action potentials at the neuron in Fig. 1A and B appear constant overtime (Fig. 1E). The constant energetic barriers for firing spikes 2–4 are generally seen at other neurons ($n = 14$ in Fig. 1F). Therefore, the inverse correlation between ARPs and Vts confers the neurons having constant energetic barriers to fire sequential action potentials, and the spike initiation in this homeostatic nature secures the fidelity of neuronal encoding.

If the energetic barrier forms a homeostatic device of neuronal encoding, it should not be deteriorated by physical and chemical manipulations. Moreover, if VGSC dynamics controls both ARP and Vts [8,10], their inverse correlation should not be dissociated by physiological manipulations. We examined these theoretical predictions under physiological conditions of causing neuronal plasticity and membrane potential change, which should indicate whether the homeostasis of neuronal encoding is always present.

We examined the effects of intracellular Ca^{2+} levels on the relationship between ARPs and Vts as well as on the energetic barrier to fire action potentials, in which cytoplasmic Ca^{2+} levels were lowered by infusing BAPTA [11] and raised by adenophostin-A [6].

Fig. 2A and B shows the effects of raising intracellular Ca^{2+} on the relationship between ARPs and Vts as well as on the energetic barrier for firing sequential spikes. Similar to the result in Fig. 1, the longer ARPs are associated with the lower Vts, or vice versa. There are linear and inverse correlations between ARP1 and Vts2 (red lines), between ARP2 and Vts3 (green), as well as between ARP3 and Vts4 (blue in Fig. 2A; $n = 12$, $r^2 > 0.85$, $p < 0.001$). The constant energetic barriers for firing spikes 2–4 are seen at these neurons ($n = 12$ in Fig. 2B). Therefore, an increase of intracellular Ca^{2+} does not affect the inverse correlation between ARPs and Vts as well as the constant energetic barrier. The homeostasis of neural encoding is maintained when intracellular Ca^{2+} rises, which may induce neuronal plasticity [6].

The effects of reducing intracellular Ca^{2+} on the relationships between ARPs and Vts as well as on the energetic barrier to fire sequential action potentials are showed in Fig. 2C and D. There are linear and inverse correlations between ARP1 and Vts2 (red lines), between ARP2 and Vts3 (green lines), as well as between ARP3 and Vts4 (blue in Fig. 2C, $n = 7$, $r^2 > 0.85$, $p < 0.001$). The energetic barriers to fire action potentials 2–4 at these neurons are constant overtime (Fig. 2D, $n = 7$). Thus, the homeostasis of neuronal

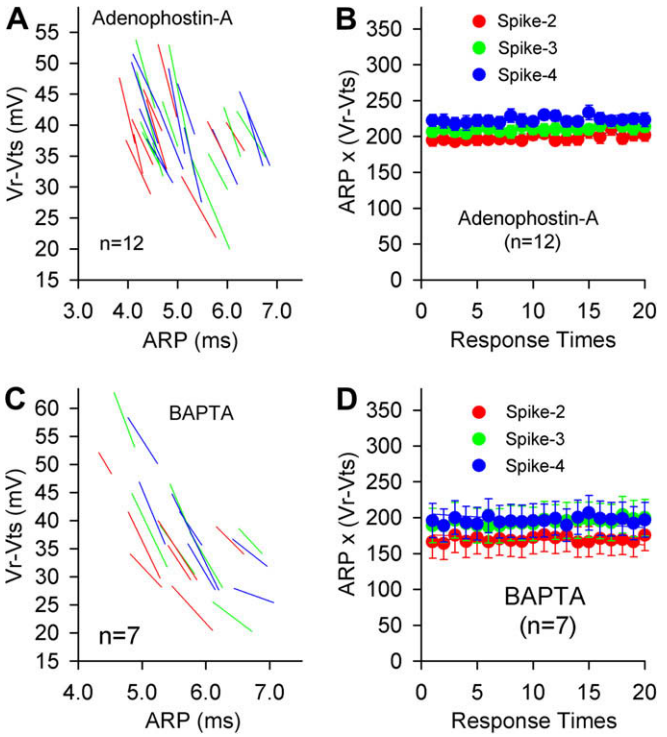

Fig. 2. The levels of intracellular Ca^{2+} do not change inverse correlation between ARP and Vts as well as constant energetic barrier for firing action potentials at GABAergic neurons. (A) The inverse correlations between ARP1 and Vts2 (red lines), ARP2 and Vts3 (green), as well as ARP3 and Vts4 (blue) during the infusions of adenophostin-A (100 μM) into the neurons ($n = 12$). (B) The energetic barrier (ARP * Vts) versus response time of spike-2 (red symbols), spike-3 (green) and spike-4 (blue) at these neurons. (C) The inverse correlations between ARP1 and Vts2 (red lines), ARP2 and Vts3 (green), as well as ARP3 and Vts4 (blue) during the infusion of BAPTA (1 mM) into the neurons ($n = 7$). (D) The energetic barrier versus response time of spike-2 (red symbols), spike-3 (green) and spike-4 (blue) from these neurons. (For interpretation of the references to color in this figure legend, the reader is referred to the web version of this paper.)

encoding is maintained when the neurons have the low level of intracellular Ca^{2+}.

We also examined the effects of membrane potentials on the ARP and Vts of sequential spikes under hyperpolarization (HP) or depolarization (DP). Fig. 3A and B shows the effects of HP about 10 mV on the relationships between ARPs and Vts as well as on the energetic barriers to fire sequential spikes. There are linear and inverse correlations between ARP1 and Vts2 (red lines), between ARP2 and Vts3 (green), as well as between ARP3 and Vts4 (blue in Fig. 3A; $n = 7$, $r^2 > 0.85$, $p < 0.001$). The energetic barriers for firing spikes 2–4 are constant at these neurons ($n = 7$ in Fig. 3B). In addition, Fig. 3C and D shows the effects of DP about 10 mV on the relationships between ARPs and Vts as well as on the energetic barriers. There are linear and inverse correlations between ARP1 and Vts2 (red lines), between ARP2 and Vts3 (green) as well as between ARP3 and Vts4 (blue in Fig. 3C, $n = 7$, $r^2 > 0.85$, $p < 0.001$). The constant trend of energetic barriers to fire spikes 2–4 is seen at these neurons (Fig. 3D, $n = 7$). Therefore, membrane potentials do not affect the inverse correlations between ARPs and Vts as well as the constant energetic barriers for firing action potentials.

These data indicate that the domains of controlling the inverse correlation between ARP and Vts as well as the constant energetic barrier to fire action potentials are not modulated by intracellular signaling pathways and membrane potential fluctuation, i.e., the homeostasis for stabilizing neuronal encoding is always present.

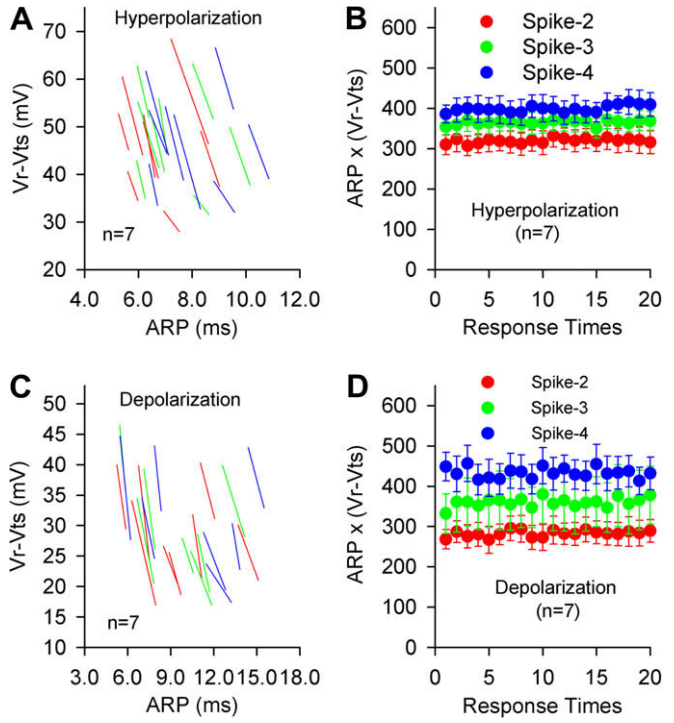

Fig. 3. The levels of membrane potentials do not change inverse correlation between ARP and Vts as well as constant energetic barrier for firing action potentials at GABAergic neurons. (A) The inverse correlations between ARP1 and Vts2 (red lines), ARP2 and Vts3 (green), as well as ARP3 and Vts4 (blue) during a hyperpolarization (HP) about 10 mV ($n = 7$). (B) The energetic barrier (ARP $*$ Vts) versus response time of spike-2 (red symbols), spike-3 (green) and spike-4 (blue) from these neurons. (C) The inverse correlations between ARP1 and Vts2 (red lines), ARP2 and Vts3 (green), as well as ARP3 and Vts4 (blue) during a depolarization (DP) about 10 mV ($n = 7$). (D) The energetic barrier versus response time of spike-2 (red symbols), spike-3 (green) and spike-4 (blue) from these neurons. (For interpretation of the references to color in this figure legend, the reader is referred to the web version of this paper.)

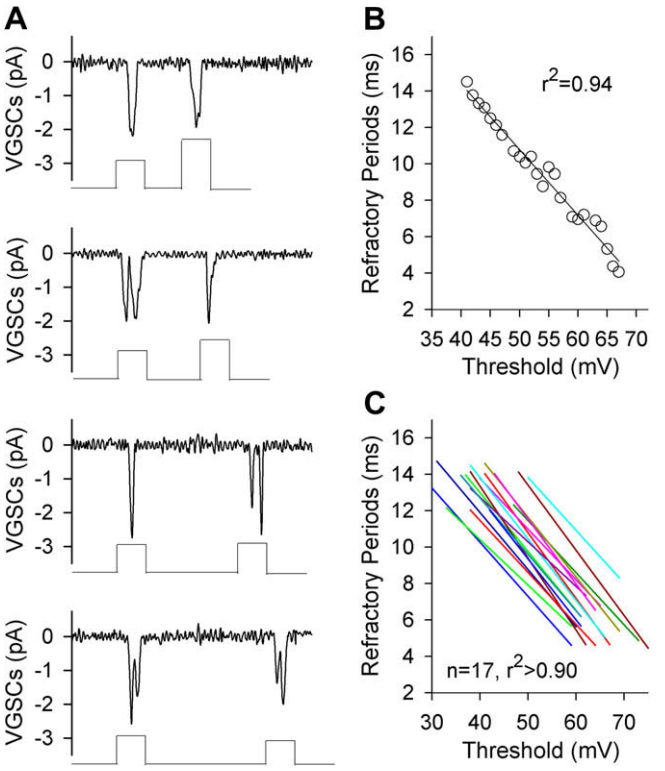

Fig. 4. VGSC refractory period and threshold potential are inversely and linearly correlated. Two depolarization pulses (5 ms) were added to patch pipettes to activate VGSCs, in which inter-pulse intervals and the second pulse amplitudes were adjusted to measure ARP for VGSC reactivation and Vts for VGSC activation. (A) show the recording of a single VGSC on a cortical neuron, in which the second pulse amplitudes decrease and inter-pulse intervals prolong from the top to the bottom panels. (B) Dots and a line show the inversely linear correlation between ARP and Vts for this VGSC in panels A ($r^2 = 0.94$, $p < 0.01$). (C) Lines show the inversely linear correlation between ARP and Vts for other VGSCs ($n = 17$; $r^2 > 0.9$, $p < 0.01$).

As ARP and Vts are under the control of VGSCs, we tested whether there is an inverse correlation between ARP and Vts of VGSCs.

We measured the refractory periods for VGSC reactivation and threshold potential for its activation by using a cell-attached configuration of patch-clamp to record single VGSCs in the cortical neurons of brain slices. Fig. 4 illustrates the ARP and Vts of VGSCs. Waveforms in Fig. 4A present currents recorded from a single VGSC, in which the shorter refractory periods appear associated with the higher threshold potentials. Fig. 4B shows that the ARP and Vts of this VGSC are inversely and linearly correlated ($r^2 = 0.94$, $p < 0.01$). These two parameters from other VGSCs are also inversely and linearly correlated (Fig. 4C, $n = 17$; $r^2 > 0.90$, $p < 0.01$). The values for the multiplication of ARP and Vts are consistent. These data indicate that refractory period for VGSC reactivation and threshold potential for VGSC activation at cortical neurons are fluctuated, and they are inversely correlated for the constant energetic barriers to initiate sequential action potentials.

Discussion

Our results reveal that threshold potential for VGSCs' activation and refractory period for their reactivation change toward the different directions synchronously, and that their inverse correlation maintains constant energetic barrier for firing sequential action potentials overtime, i.e., a homeostasis of neuronal encoding. This stabilization of neuronal functions in real-time manner is a novel type of cellular homeostasis, compared to other types by influencing gene expression in a feedback manner [1,2] and by coordinating subcellular compartments in a feedforward manner [6]. As this homeostasis of VGSC-mediated neuronal encoding is not influenced by membrane potentials and cytoplasmic Ca^{2+} signals, this natural mechanism is present intrinsically in VGSCs. It remains to be tested whether other molecules influence the homeostasis of cellular functions through a similar process.

In the brain, homeostasis precludes the disturbance of internal environmental changes to neuronal functions. Homeostasis also prevents the neurons from the loss of functions that are established during development and postnatal experience. Therefore, neuronal homeostasis in signal encoding and other functions may signify the memory imprints in the cells, a cellular mechanism for learning and memory.

The onsets of homeostasis at different times play distinct roles in stabilizing neuronal functions. Slowly-onset homeostasis by up or down-regulating gene expression compensates initial changes in neuronal activities [1,3–5,12,13]. Gene expression and subsequent protein synthesis make neuronal activities slowly stabilized and the neurons overly active when the initial factors are removed [3]. Second, Ca^{2+}-mediated homeostatic coordination of subcellular compartments is initiated and removed associatively without the need of gene expression, which is a rapid and efficient process to minimize the instability of neuronal encoding during the plasticity [6]. Third, VGSC-mediated homeostasis of firing action potentials

makes a molecule to set its intrinsic properties toward different directions synchronously and stabilize neuronal encoding. Therefore, three types of homeostatic mechanisms are sequentially initiated and physiologically needed to stabilize brain functions.

Based on the studies of homeostasis up to date, we classify the mechanisms underlying cellular homeostasis into real-time homeostasis and homeostatic plasticity. The real-time homeostasis by regulating the intrinsic properties of a molecule maintain neuronal encoding to be precise and reliable without any interruption, whereas the homeostatic plasticity takes homeostatic neuronal encoding back via the plasticity among subcellular compartments or in gene expression. Therefore, it is physiologically present that the neurons in the brain encode precise and reliable messages for the well-organized cognition and behavior. A real-time regulation in the homeostasis of neuronal encoding is essentially needed for brain functions. In addition to real-time homeostasis in spike encoding we present, other types of neuronal homeostasis in synchronous regulation remain to be investigated.

Although the energetic barriers to initiate sequential spikes are stable (i.e., homeostasis in neuronal encoding), spiking thresholds and refractory periods are fluctuated (Fig. 1). This indicates that the stabilization in neural events is established on dynamical balance among multiple neuronal properties, which relies on the certain unidentified organizers (coupling or signaling molecules). Neuronal threshold [14] and synapse dynamics [15] have been found to be fluctuated. When the organizers convert their fluctuated patterns into uniform, neuronal encoding will be more stable and efficient [15]. If these fluctuated intrinsic properties in the neurons and synapses are not well-organized, their dissociation will result in functional disorders in the brain.

The homeostasis of neuronal encoding in our study needs a synchronous regulation of VGSC refractory period and threshold potential in a manner of inverse correlation. As this featured regulation is not influenced by membrane potentials and intracellular Ca^{2+} signals, the domain in VGSCs that regulates ARP and Vts coordinately is most likely structured in the inside of molecules. This domain, we called as an organizer of ARP and Vts, differs from the domains of setting ARP and Vts that are regulated by signaling pathways and input intensity [6,15]. The location of such domains in VGSCs remains to be elucidated by functional structure biology.

Here, we present a novel type of homeostasis for neuronal encoding that is fulfilled by simultaneously regulating refractory period for VGSC reactivation and threshold potential for its activation in an inverse manner to set constant energetic barrier for firing sequential action potentials, which is able to stabilize neuronal excitability and spike encoding.

Acknowledgements

Ge and Chen contributed to experimental works. This study is granted by the National Award for Outstanding Young Scientist (30325021), National Basic Research Program (2006CB500804), Natural Science Foundation China (30621130077 and 30870517), CAS Program for Knowledge Innovation (KSCX2-YWR-39) to J.H.W. Except for providing research funds, funders have no role in experimental design and data publication.

References

[1] J. Burrone, V. Murthy, Synaptic gain control and homeostasis, Current Opinion in Neurobiology 13 (2003) 560–567.
[2] G.G. Turrigiano, S. Nelson, Homeostatic plasticity in the developing nervous system, Nature Reviews Neuroscience 5 (2004) 97–107.
[3] N.S. Desai, L. Rutherford, G.G. Turrigiano, Plasticity in the intrinsic excitability of cortical pyramidal neurons, Nature Neurosciences 2 (6) (1999) 515–520.
[4] G.J. Ramakers, M.A. Corner, A.M. Habers, Development in the absence of spontaneous bioelectric activity results in increased stereotyped burst firing in cultures of associated cerebral cortex, Experimental Brain Research 79 (1990) 157–166.
[5] A.N. Van Den Pol, K. Obrietan, A. Belousov, Glutamate hyperexcitability and seizure-like activity throughout the brain and spinal cord upon relief from chronic glutamate receptor blockade in culture, Neuroscience 74 (1996) 653–674.
[6] N. Chen, X. Chen, J.-H. Wang, Homeostasis established by coordination of subcellular compartment plasticity improves spike encoding, Journal of Cell Science 121 (17) (2008) 2961–2971.
[7] N. Chen, S.L. Chen, Y.L. Wu, J.H. Wang, The refractory periods and threshold potentials of sequential spikes measured by whole-cell recordings, Biochemical and Biophysical Research Communications 340 (2006) 151–157.
[8] N. Chen, Y. Zhu, X. Gao, S. Guan, J.-H. Wang, Sodium channel-mediated intrinsic mechanisms underlying the differences of spike programming among GABAergic neurons, Biochemical and Biophysical Research Communications 346 (2006) 281–287.
[9] J.-H. Wang, Short-term cerebral ischemia causes the dysfunction of interneurons and more excitation of pyramidal neurons, Brain Research Bulletin 60 (1–2) (2003) 53–58.
[10] N. Chen, X. Chen, J. Yu, J.-H. Wang, After-hyperpolarization improves spike programming through lowering threshold potentials and refractory periods mediated by voltage-gated sodium channels, Biochemical and Biophysical Research Communications 346 (2006) 938–945.
[11] R.Y. Tsien, New calcium indicators and buffers with high selectivity against magnesium and protons: design, synthesis, and properties of prototype structures, Biochemistry 19 (11) (1980) 2396–2404.
[12] M.D. Ehlers, Activity level controls postsynaptic composition and signaling via the ubiquitin–proteasome system, Nature Neuroscience 6 (2003) 231–242.
[13] I. Perez-Otano, M.D. Ehlers, Homeostatic plasticity and NMDA receptor trafficking, Trends in Neurosciences 28 (5) (2005) 229–238.
[14] R. Azous, C.M. Gray, Dynamic spike threshold reveals a mechanism for synaptic coincidence detection in cortical neurons in vivo, Proceeding of National Academy of Sciences United States of America 97 (14) (2000) 8110–8115.
[15] J.H. Wang, J. Wei, X. Chen, J. Yu, N. Chen, J. Shi, The gain and fidelity of transmission patterns at cortical excitatory unitary synapses improve spike encoding, Journal of Cell Science 121 (17) (2008) 2951–2960.